

# Rhodium Supported on Silica-Stabilized Alumina for Catalytic Decomposition of N<sub>2</sub>O

Xiangyun Zhao · Yu Cong · Yanqiang Huang ·  
Shuang Liu · Xiaodong Wang · Tao Zhang

Received: 7 September 2010 / Accepted: 12 October 2010 / Published online: 2 November 2010  
© Springer Science+Business Media, LLC 2010

**Abstract** Silica-stabilized alumina calcined at 1200 °C has been used as a support for rhodium catalysts, and tested in catalytic decomposition of N<sub>2</sub>O propellant. Significant enhancement of catalytic performance was obtained on the silica-stabilized catalyst owing to the thermally stable structure favoring the stabilization of Rh<sup>0</sup> species and desorption of oxygen during the decomposition process.

**Keywords** Nitrous oxide · Rhodium · Decomposition · Al<sub>2</sub>O<sub>3</sub> · SiO<sub>2</sub>

## 1 Introduction

Nitrous oxide (N<sub>2</sub>O) has received growing interest as a promising green propellant for small satellite propulsion due to its low toxicity, self pressurizing, and multi-mode propulsion [1, 2]. The earlier successful experiences of using N<sub>2</sub>O as a propellant within a resisto-jet propulsion system on the UoSAT-12 mini-satellite and as the oxidizer for the hybrid engine powering “Spaceship One” have shown the great potential and feasibility of N<sub>2</sub>O as a green propellant for modern advanced propulsions. However,

thermal decomposition of gaseous N<sub>2</sub>O requires high power input due to the high activation energy of ca. 250 kJ/mol, and it leads to a temperature rise over 1000 °C because of its highly exothermic nature. Therefore, there is an urgent need to develop novel catalyst materials which possess high catalytic activities at low temperatures and thermal stabilities at high temperatures for N<sub>2</sub>O propellant applications.

Alumina has been widely used as a catalyst or catalyst supports due to its large surface area, tunable surface property, and suitable interaction with the active metal components. There have been some reports about the alumina-supported metal catalysts for the decomposition of N<sub>2</sub>O propellant. For example, Wallbank et al. [3] reported that Shell 405 (36 wt% Ir/Al<sub>2</sub>O<sub>3</sub>) exhibited a high activity in the decomposition of N<sub>2</sub>O propellant. Zakirov et al. [4] investigated more than 50 different catalysts for the decomposition of pure N<sub>2</sub>O for small spacecraft propulsion, and found that Rh/Al<sub>2</sub>O<sub>3</sub> had the highest turnover frequency.

On the other hand, it is known that  $\gamma$ -Al<sub>2</sub>O<sub>3</sub> is unstable in high-temperature processes; phase transformation from  $\gamma$ -Al<sub>2</sub>O<sub>3</sub> to  $\alpha$ -Al<sub>2</sub>O<sub>3</sub> often occurs at above 1000 °C accompanied with a dramatic decrease in surface area, which results in severe deactivation of the catalysts. Therefore, it is of vital importance to improve the thermal stability of alumina support for the catalytic decomposition of N<sub>2</sub>O propellant. Addition of promoters to alumina is an effective method for suppressing the surface area loss and avoiding transition to  $\alpha$ -Al<sub>2</sub>O<sub>3</sub> induced by high-temperature reactions [5–13]. Beguin et al. [9] reported that numerous cations, such as La<sup>3+</sup>, Zr<sup>3+</sup>, Ca<sup>2+</sup>, and Th<sup>4+</sup>, were extremely effective for retarding the sintering and phase transformation of alumina at high temperatures. Courthéoux et al. [10] prepared silica-doped alumina

**Electronic supplementary material** The online version of this article (doi:10.1007/s10562-010-0472-3) contains supplementary material, which is available to authorized users.

X. Zhao · Y. Cong · Y. Huang · S. Liu · X. Wang ·  
T. Zhang (✉)  
State Key Laboratory of Catalysis, Dalian Institute of Chemical  
Physics, CAS, Dalian 116023, People’s Republic of China  
e-mail: taozhang@dicp.ac.cn

X. Zhao · S. Liu  
Graduate School of the Chinese Academy of Sciences, Beijing  
100049, People’s Republic of China

aerogels by a sol–gel method and demonstrated a marked increase in the thermal stability after calcination at 1200 °C, owing to silicon atoms stabilizing the alumina defect structure. Osaki et al. [13] also found that silica-doped alumina cryogels exhibited a high thermal stability by virtue of the synergetic effects of the very low bulk density and the dopant. These previous studies have shown that doping alumina with silicon atoms could improve the thermal stability of the materials. However, it is unknown if such doping process is helpful in promoting the activity at low reaction temperatures because the doping process also causes changes of surface properties which will influence the chemical states of the adsorbed metal particles.

Previously, we reported that mullite, a type of ceramic material with the chemical composition of  $3\text{Al}_2\text{O}_3 \cdot 2\text{SiO}_2$ , was a very good support of Rh catalysts in the decomposition of  $\text{N}_2\text{O}$  propellant [14]. More interestingly, the low-temperature activity was also enhanced together with the remarkably improved high-temperature stability as a result of the formation of mullite. In the present work, we prepared a series of silica-stabilized alumina materials with different silica concentrations, and investigated their catalytic performances for the catalytic decomposition of  $\text{N}_2\text{O}$  propellant. The promotional effect of silicon-doping was also studied in detail by using a variety of characterization techniques.

## 2 Experimental

### 2.1 Catalyst Preparation

The silica-stabilized alumina samples were prepared by co-precipitation method, using  $\text{Al}(\text{NO}_3)_3 \cdot 9\text{H}_2\text{O}$  and tetraethylorthosilicate (TEOS) as starting reactants and  $(\text{NH}_4)_2\text{CO}_3$  as a precipitant. In a typical synthesis, 2.1 g of TEOS was dissolved in 10 mL ethanol, and this ethanol solution was mixed with 50 mL of an aqueous solution of aluminum nitrate (1 mol/L). To the above mixed solution, 20 mL of an aqueous solution of  $(\text{NH}_4)_2\text{CO}_3$  (5 mol/L) was added and followed by vigorous stirring at 60 °C for 3 h. The precipitate was then filtered, dried at 120 °C for 64 h, and calcined in air at 1200 °C for 4 h. The concentration of  $\text{SiO}_2$  in this sample was 19 wt%, and denoted as  $\text{Si}_{0.19}\text{Al}$ . For comparison, samples with concentrations of  $\text{SiO}_2$  of 5 and 32 wt% were also prepared with the same procedure, and denoted as  $\text{Si}_{0.05}\text{Al}$  and  $\text{Si}_{0.32}\text{Al}$ , respectively. In some cases, the  $\text{Si}_{0.19}\text{Al}$  sample was calcined at different temperatures (T), and denoted as  $\text{Si}_{0.19}\text{Al-T}$ .

To investigate the effect of different dopants,  $\text{La}_2\text{O}_3$ -,  $\text{CeO}_2$ -, and  $\text{ZrO}_2$ -doped alumina samples were also

prepared by co-precipitation with  $\text{La}(\text{NO}_3)_3 \cdot 6\text{H}_2\text{O}$ ,  $\text{Ce}(\text{NO}_3)_3 \cdot 6\text{H}_2\text{O}$ , and  $\text{Zr}(\text{NO}_3)_3 \cdot 4\text{H}_2\text{O}$  as the precursors of dopants, and denoted as  $\text{La}_{0.19}\text{Al}$ ,  $\text{Ce}_{0.19}\text{Al}$ , and  $\text{Zr}_{0.19}\text{Al}$ , respectively.

The Rh-supported catalysts were prepared by incipient wetness impregnation of the above-prepared supports with an aqueous solution of  $\text{RhCl}_3$  to give a calculated Rh loading of 4.4 wt%. The catalysts were calcined at 500 °C for 4 h. For comparison,  $\text{Rh}/\gamma\text{-Al}_2\text{O}_3$  was also prepared with the same procedure.

Finally, in order to investigate the thermal stability of the catalysts, the prepared catalysts were further calcined at 1200 °C for 4 h, yielding the catalysts named as 1200-Rh/ $\text{Si}_x\text{Al}$  and 1200-Rh/ $\text{Al}_2\text{O}_3$ .

### 2.2 Catalyst Characterization

BET surface areas of the catalysts were measured by  $\text{N}_2$  adsorption at  $-196$  °C using a Micromeritics ASAP 2010 apparatus. The X-ray diffraction (XRD) patterns were recorded with a PANalytical X'Pert-Pro powder X-ray diffractometer, using Cu  $K\alpha$  monochromatized radiation ( $\lambda = 0.1541$  nm) at a scan speed of 5°/min.

Rh dispersion was derived from the measurement of  $\text{H}_2$  chemisorption uptake at room temperature using a Micromeritics AutoChem 2090 apparatus. Before each experiment, catalysts were reduced with  $\text{H}_2$  at 500 °C for 2 h. Temperature programmed reduction (TPR) experiments were carried out on the same apparatus. 100 mg of a catalyst was loaded into a U-shape quartz reactor and pretreated in Ar at 500 °C for 2 h. The samples were cooled to room temperature and then the flowing gas was switched to a 10 vol%  $\text{H}_2/\text{Ar}$ . The catalysts were heated to 500 °C at a ramping rate of 10 °C/min.

Oxygen adsorption experiments were performed with a BT2.15 heat-flux calorimeter. Prior to the measurement, catalyst was preheated in a special treatment quartz cell in  $\text{H}_2$  from room temperature to 500 °C and held at that temperature for 2 h. Then, the sample was outgassed in situ in high vacuo ( $3 \times 10^{-4}$  Pa) at 500 °C for 0.5 h. The microcalorimetric data were collected by sequentially introducing small doses (1–10  $\mu\text{mol}$ ) of  $\text{O}_2$  onto the sample until it became saturated (5–6 Torr).

Transmission infrared spectra were obtained with a Bruker Equinox 55 spectrometer at a resolution of  $4\text{ cm}^{-1}$  using 64 scans. The self-supporting wafers (14 mg) were prepared and placed in an IR cell with NaCl windows and a temperature controller. Each sample was pretreated with  $\text{H}_2$  at 500 °C for 45 min and then evacuated at that temperature for 15 min. The CO adsorption was carried out at room temperature under 3 Torr CO. The spectra were recorded ca. 10 min after CO adsorption.

### 2.3 Catalytic Activity Tests

Catalytic decomposition of  $N_2O$  over supported rhodium catalysts was carried out in a fix-bed flow reactor system at atmospheric pressure. 0.1 g of a catalyst (20–40 mesh in particle size) was mixed with 0.40 g of quartz to prevent temperature gradient, and loaded in a silica glass tube reactor of 6 mm i.d. with silica wool. The reaction temperature was measured by thermocouples located at the inlet of the catalyst bed. Prior to each run, the catalysts were in situ reduced with  $H_2$  at 500 °C for 2 h. The reacting gas containing  $N_2O$  (30 vol%) in Ar was then introduced in the reactor at a flow rate of 50 mL/min. Reactant and product concentrations were measured by on-line gas chromatography (Agilent GC-6890N) with a Porapak Q column (for  $N_2O$ ) and a 13 X column (for  $N_2$  and  $O_2$ ).  $N_2$  and  $O_2$  were identified as the only products (Fig. S1).  $N_2O$  conversion was determined based on the difference between its inlet and outlet concentrations.

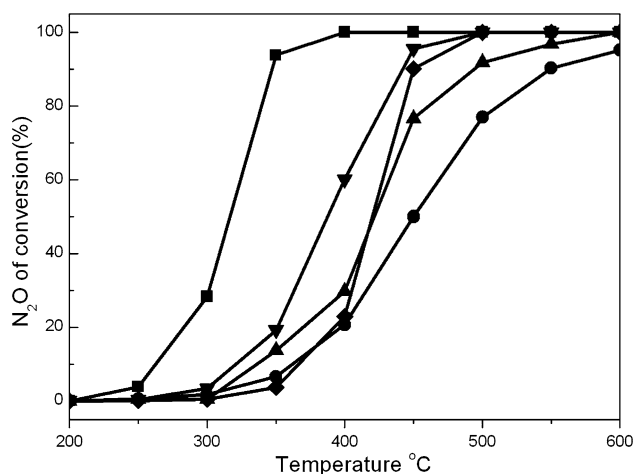
## 3 Results and Discussion

### 3.1 Metal Oxide-Stabilized Alumina as Support for Rhodium Catalysts

Figure 1 compares the  $N_2O$  conversions as a function of reaction temperature over metal oxide-stabilized alumina supported rhodium catalysts. The referenced sample,  $Rh/\gamma-Al_2O_3$ , exhibited a reasonable activity compared to what have ever been reported under the same reaction conditions [14–16]. Decomposition started at 300 °C and complete decomposition was attained at 500 °C. After metal oxides of Si, La, Zr, and Ce were introduced, the resulting catalysts exhibited different catalytic activities in  $N_2O$  decomposition. The  $Rh/Si_{0.19}Al$  showed the highest activity, shifting the  $N_2O$  conversion curve toward a lower temperature of 100 °C. The  $Rh/La_{0.19}Al$  catalyst also showed a slight increase in activity, especially in the low temperature range. In contrast, the  $Rh/Zr_{0.19}Al$  and  $Rh/Ce_{0.19}Al$  samples demonstrated even lower activities than the  $Rh/\gamma-Al_2O_3$ . Obviously, introducing metal oxides to the alumina support has a significant influence on its characteristics as well as the subsequent catalyst. Therefore, further studies into the understanding of the doping effect are of great importance. With a view to the most obvious promotion effect in the decomposition,  $SiO_2$  was selected as the doping material for the following research.

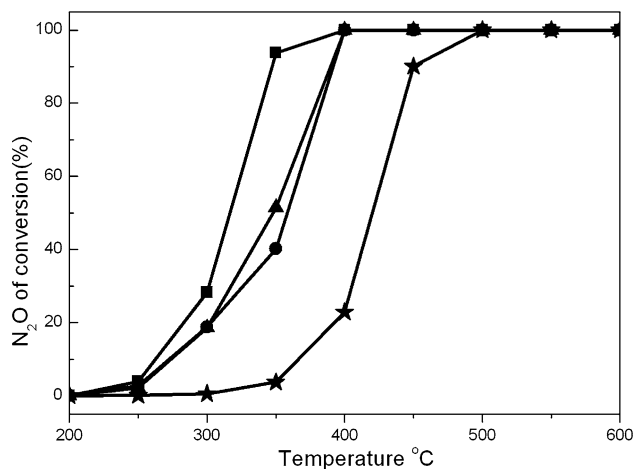
### 3.2 Effect of the Si Content

Figure 2 illustrates the  $N_2O$  conversion of the  $Rh/Si_xAl$  catalysts with different silica content. It can be seen that



**Fig. 1**  $N_2O$  conversion as a function of temperature over the  $Rh/M_xAl$  catalysts:  $Rh/Si_{0.19}Al$  (filled square),  $Rh/La_{0.19}Al$  (filled inverted triangle),  $Rh/Zr_{0.19}Al$  (filled triangle),  $Rh/Ce_{0.19}Al$  (filled circle), and  $Rh/\gamma-Al_2O_3$  (filled diamond) (the  $M_xAl$  supports were calcined at 1200 °C, while  $\gamma-Al_2O_3$  was calcined at 500 °C)

even a small amount of silica had a significant promotion effect on the catalytic activity. For example, the  $Rh/Si_{0.05}Al$  catalyst showed a much higher activity than the  $Rh/\gamma-Al_2O_3$ , starting the decomposition at 200 °C and reaching 53%  $N_2O$  conversion at 350 °C. The silica content affected the  $N_2O$  conversion in the following sequence:  $Rh/\gamma-Al_2O_3 < Rh/Si_{0.32}Al < Rh/Si_{0.05}Al < Rh/Si_{0.19}Al$ . Clearly, it appeared that there was an optimum amount of silica for the  $Rh/Si_xAl$  catalysts in the decomposition of  $N_2O$ . In the present work, the  $Rh/Si_{0.19}Al$  was assumed to possess the best chemical composition for the limited catalysts studied.



**Fig. 2**  $N_2O$  conversion as a function of temperature over the  $Rh/Si_xAl$  catalysts with different silica content:  $Rh/Si_{0.19}Al$  (filled square),  $Rh/Si_{0.05}Al$  (filled triangle),  $Rh/Si_{0.32}Al$  (filled circle),  $Rh/\gamma-Al_2O_3$  (filled asterisk)

**Table 1** Physicochemical properties of the Rh/Si<sub>x</sub>Al and Rh/γ-Al<sub>2</sub>O<sub>3</sub> catalysts

Sample	S <sub>BET</sub> (m <sup>2</sup> /g)			Rh content <sup>c</sup> (wt%)	Dispersion (%)	
	Support	Fresh cat.	Used cat.		Fresh cat.	Used cat.
Rh/Si <sub>0.32</sub> Al <sup>a</sup>	50	47	46	4.07	46	–
Rh/Si <sub>0.19</sub> Al <sup>a</sup>	55	53	51	4.03	45	41
Rh/Si <sub>0.05</sub> Al <sup>a</sup>	57	55	54	4.05	43	–
Rh/γ-Al <sub>2</sub> O <sub>3</sub> <sup>b</sup>	265	253	244	4.01	83	79

<sup>a</sup> The support calcined at 1200 °C, the final catalyst calcined at 500 °C

<sup>b</sup> The support calcined at 500 °C, the final catalyst calcined at 500 °C

<sup>c</sup> Determined by inductively coupled plasma (ICP) atomic emission spectrometry

The BET surface areas of the supports, fresh catalysts, and used catalysts are summarized in Table 1. A slight decrease in BET surface areas of the supports after depositing rhodium was observed on all the samples, which may be caused by the blockage of some pores by rhodium. Rh dispersions increased with increasing the BET surface areas. The γ-Al<sub>2</sub>O<sub>3</sub> calcined at 500 °C had the highest specific surface area of 265 m<sup>2</sup>/g, and the highest Rh dispersion of 83% in accordance. After calcination at 1200 °C, α-Al<sub>2</sub>O<sub>3</sub> was formed accompanied with a marked surface area loss to about 7 m<sup>2</sup>/g. In contrast, the silica-stabilized samples possessed rather high surface area (above 50 m<sup>2</sup>/g) after calcination at the same temperature of 1200 °C. We also examined the BET surface areas and Rh dispersions of the catalysts after activity test. No significant modification of the support and active phase occurred during the course of the experiment (Figs. S2, S3). In correlation with the catalytic performances above, we could propose that the BET surface area and the active component dispersion are not primary parameters for the activity enhancement. The modification of the support properties by doping silica probably played a key role on the decomposition of N<sub>2</sub>O.

XRD patterns of the Si<sub>x</sub>Al supports appear in Fig. 3. For the Si<sub>0.05</sub>Al and Si<sub>0.32</sub>Al samples, the typical diffraction peaks of θ-Al<sub>2</sub>O<sub>3</sub> were detected along with traces of α-Al<sub>2</sub>O<sub>3</sub>. While in the case of Si<sub>0.19</sub>Al, it appeared only the peaks of θ-Al<sub>2</sub>O<sub>3</sub>. According to the previous work, the γ-Al<sub>2</sub>O<sub>3</sub> was completely transformed into α-Al<sub>2</sub>O<sub>3</sub> during the thermal treatment at 1200 °C [14]. Clearly, the addition of 19 wt% silica strongly suppressed the phase transformation of alumina from θ to α. To be noted, the phase transformation of transition alumina is a process of dehydroxylation, resulting in the generation of oxygen vacancies [17, 18]. To be noted, among the different types of alumina (γ, δ, θ, α), oxygen vacancies are thought to be most abundant in the θ-Al<sub>2</sub>O<sub>3</sub> [17]. It has been generally accepted that oxygen desorption is the rate determining step during N<sub>2</sub>O decomposition [19]. Therefore, the oxygen vacancies on the support are believed favorable for the

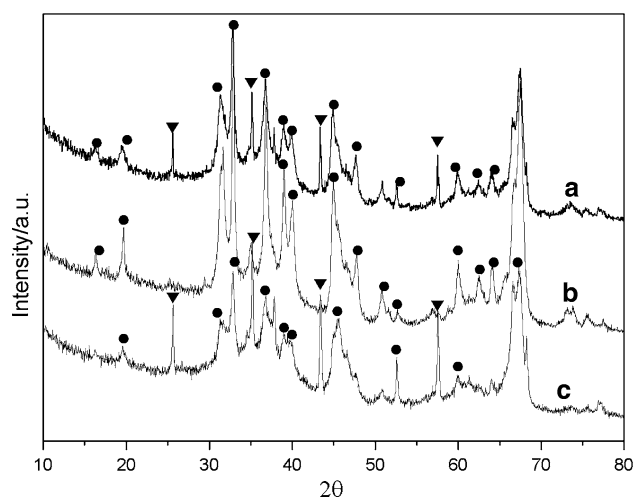


**Fig. 3** XRD patterns of the Si<sub>x</sub>Al supports calcined at 1200 °C: Si<sub>0.05</sub>Al (a), Si<sub>0.19</sub>Al (b), Si<sub>0.32</sub>Al (c); α-Al<sub>2</sub>O<sub>3</sub> (filled inverted triangle), θ-Al<sub>2</sub>O<sub>3</sub> (filled circle)

mobility of oxygen derived from N<sub>2</sub>O decomposition, which led to the superior activity of the Rh/Si<sub>0.19</sub>Al catalyst, in agreement with a previous report [20]. In order to verify the above proposition, we also tested the effect of calcination temperature of alumina support on the performance of Rh catalysts supported thereof. As shown in Fig. 4, a gradual improvement of the catalytic performance was also observed when the calcination temperature was raised from 500 to 1100 °C. XRD patterns of the Al<sub>2</sub>O<sub>3</sub>-1100 sample indicated that there existed a significant amount of θ-Al<sub>2</sub>O<sub>3</sub> after calcination at 1100 °C, as illustrated in supplementary Fig. S4. This result further confirmed that the formation of θ-Al<sub>2</sub>O<sub>3</sub> contributes significantly to the enhanced activity, as discussed above.

Another possibility connecting the high performance on the Rh/Si<sub>0.19</sub>Al may involve the reducibility of the rhodium. H<sub>2</sub>-TPR technique is known as a useful tool for gauging this property. Each TPR profile in Fig. 5 showed only a single reduction peak, which could be assigned to the reduction of Rh [21]. The rhodium on the SiO<sub>2</sub>

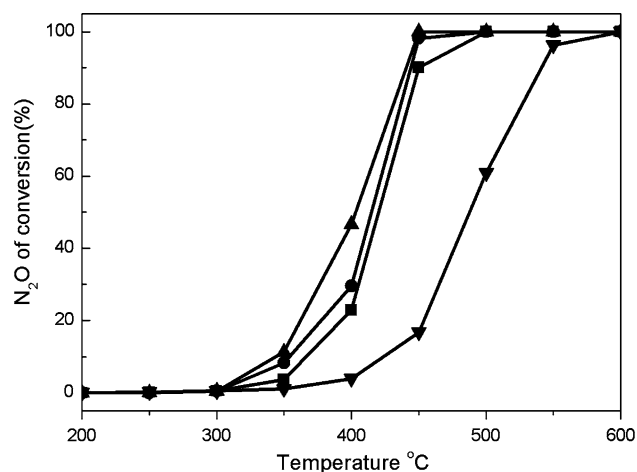


**Fig. 4** N<sub>2</sub>O conversion as a function of temperature over the Rh/Al<sub>2</sub>O<sub>3</sub>-T catalysts: Rh/Al<sub>2</sub>O<sub>3</sub>-500 (filled square), Rh/Al<sub>2</sub>O<sub>3</sub>-1000 (filled circle), Rh/Al<sub>2</sub>O<sub>3</sub>-1100 (filled triangle), Rh/Al<sub>2</sub>O<sub>3</sub>-1200 (filled inverted triangle)

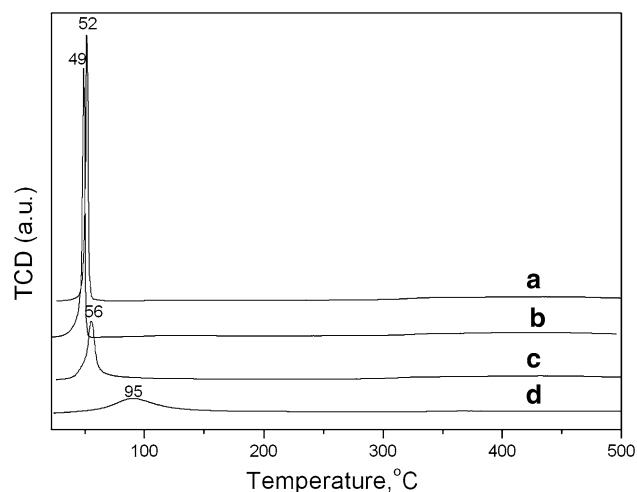


**Fig. 5** H<sub>2</sub>-TPR profiles of the Rh/Si<sub>x</sub>Al catalysts with different silica content: Rh/Si<sub>0.19</sub>Al (a), Rh/Si<sub>0.32</sub>Al (b), Rh/Si<sub>0.05</sub>Al (c), Rh/γ-Al<sub>2</sub>O<sub>3</sub> (d) (the M<sub>x</sub>Al supports were calcined at 1200 °C, while γ-Al<sub>2</sub>O<sub>3</sub> was calcined at 500 °C)

stabilized supports, with the reduction peaks below 56 °C, were more easily to be reduced compared with that on the alumina (95 °C). As has been mentioned before [14], the easy reduction of Rh species may closely correlate with the appearance of oxygen vacancies. According to literatures, it is generally believed that N<sub>2</sub>O decomposition takes place via a redox cycle [19, 20]. Therefore, the Rh<sup>0</sup> species involve a redox cycle according to the following steps:



The easily reduced rhodium species is in favor of the stability of active center in N<sub>2</sub>O decomposition, which leads to a great enhancement of catalytic activity.

### 3.3 Effect of Calcination Temperature of the Si<sub>0.19</sub>Al Support

In general, the crystal phase of alumina changes with increasing temperature in the following order:  $\gamma \rightarrow \delta \rightarrow \theta \rightarrow \alpha$ . To detect the effect of alumina phase structure on the catalytic activity of N<sub>2</sub>O decomposition, the Si<sub>0.19</sub>Al precursor was calcined at different temperatures. Figure 6 shows the effect of calcination temperature of supports on the catalytic activity of the catalysts. A gradual improvement of the catalytic performance was observed with increase of the calcination temperature. The Rh/Si<sub>0.19</sub>Al-500 has almost the same activity as the Rh/γ-Al<sub>2</sub>O<sub>3</sub>, with the temperature for complete N<sub>2</sub>O decomposition as high as 500 °C. The Rh/Si<sub>0.19</sub>Al-1200 catalyst was most active, indicating the onset of decomposition at about 200 °C and 93% of N<sub>2</sub>O conversion at 350 °C. The behaviors of the Rh/Si<sub>0.19</sub>Al-800 and Rh/Si<sub>0.19</sub>Al-1000 catalysts are intermediate, and the Rh/Si<sub>0.19</sub>Al-800 is less active than the Rh/Si<sub>0.19</sub>Al-1000. Clearly, the thermal treatment before metal deposition affected remarkably the catalytic activity of the rhodium catalysts.

Table 2 illustrates the BET surface areas of the Si<sub>0.19</sub>Al precursor calcined at different temperatures, the fresh catalysts, and the used catalysts, as well as Rh dispersion data. The Si<sub>0.19</sub>Al-500 had the largest surface area of 444 m<sup>2</sup>/g. A further increase of calcination temperature of the support to 1200 °C induced a decrease in surface area to a

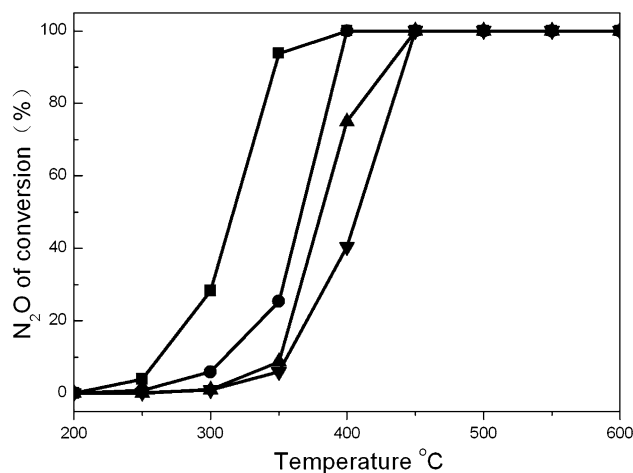


**Fig. 6** N<sub>2</sub>O conversion as a function of temperature over the Rh/Si<sub>0.19</sub>Al-T catalysts: Rh/Si<sub>0.19</sub>Al-500 (filled inverted triangle), Rh/Si<sub>0.19</sub>Al-800 (filled triangle), Rh/Si<sub>0.19</sub>Al-1000 (filled circle), Rh/Si<sub>0.19</sub>Al-1200 (filled square)



**Table 2** Physicochemical properties of Rh/Si<sub>0.19</sub>Al-T catalysts

Sample	BET surface area (m <sup>2</sup> /g)			H <sub>2</sub> consumption <sup>a</sup> (μmol/g cat)	Dispersion (%)
	Support	Fresh cat.	Used cat.		
Rh/Si <sub>0.19</sub> Al-500	444	431	418	426	89
Rh/Si <sub>0.19</sub> Al-800	178	170	162	434	79
Rh/Si <sub>0.19</sub> Al-1000	144	138	131	452	68
Rh/Si <sub>0.19</sub> Al-1200	55	53	51	481	45

<sup>a</sup> Determined by H<sub>2</sub>-TPR

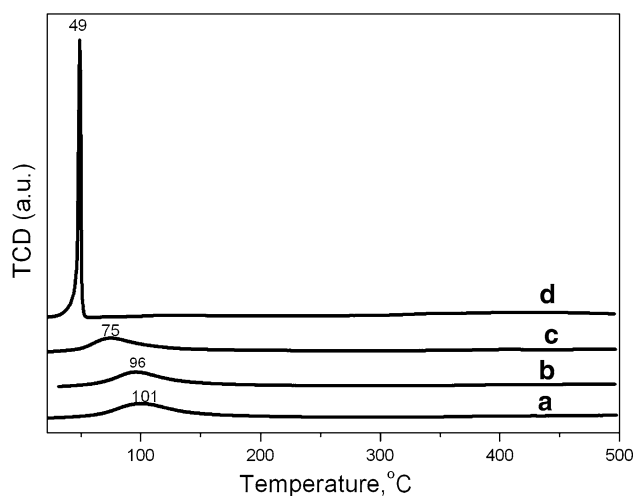


**Fig. 7** H<sub>2</sub>-TPR profiles of the Rh/Si<sub>0.19</sub>Al catalysts: Rh/Si<sub>0.19</sub>Al-500 (a), Rh/Si<sub>0.19</sub>Al-800 (b), Rh/Si<sub>0.19</sub>Al-1000 (c), Rh/Si<sub>0.19</sub>Al-1200 (d)

minimum value of 55 m<sup>2</sup>/g. It is also observed that the Rh dispersion decreased monotonously with the elevation of the calcination temperatures, which is in contrary to the trend of the catalytic activity. Apparently, the N<sub>2</sub>O decomposition activity of the Rh/Si<sub>x</sub>Al catalyst does not depend on the BET surface area of the support and the Rh dispersion, in agreement with the above results.

Influence of calcination temperature of the support on the reduction behaviors of Rh species were also investigated by H<sub>2</sub>-TPR, as shown in Fig. 7. Rh/Si<sub>0.19</sub>Al catalysts gave one reduction peak which corresponds to the reduction of oxidized Rh to metallic Rh, the same as the previous results. It should be noted that the increase of calcination temperature of the support caused an increase in the reducibility of rhodium, with lower temperatures and higher amount of H<sub>2</sub> consumption (Table 2), which may be related to the change of support structure during phase transformation. After the calcination at 1200 °C, the Si<sub>0.19</sub>Al displayed the  $\theta$ -Al<sub>2</sub>O<sub>3</sub> structure, which contains the most abundant oxygen vacancies. Thus, the Rh/Si<sub>0.19</sub>Al-1200 sample showed better reducibility than the Rh/Si<sub>0.19</sub>Al-500 one. By comparing the TPR results of the catalysts with the catalytic activity, it is worthy of noting that the easily reduced rhodium oxide should be

responsible for the enhanced activity of the Rh/Si<sub>0.19</sub>Al-T catalysts, again exemplified the assumption above.

### 3.4 IR and O<sub>2</sub> Adsorption Microcalorimetry Characterization of the Rh/Si<sub>0.19</sub>Al Catalyst

The promotion effect of silica doping on the N<sub>2</sub>O decomposition was studied in more detail by IR and O<sub>2</sub> adsorption microcalorimetry characterization on the Rh/Si<sub>0.19</sub>Al catalyst. The Rh species existed in the oxidation state on the as-prepared Rh/Si<sub>0.19</sub>Al and Rh/Al<sub>2</sub>O<sub>3</sub> catalysts. The IR spectra of CO adsorption at 298 K on the Rh/Si<sub>0.19</sub>Al catalyst reduced by H<sub>2</sub>, and pre-oxidized by N<sub>2</sub>O are shown in Fig. 8A. For the reduced sample, there were four bands, located at 2097, 2069, 2028, and 1881 cm<sup>-1</sup>, clearly observed on the Rh/Si<sub>0.19</sub>Al catalyst. The twin bands at 2097 and 2028 cm<sup>-1</sup> are attributed to the symmetric and anti-symmetric stretching mode, respectively, of Rh<sup>δ+</sup>(CO)<sub>2</sub> species, as already evidenced by previous reports [22–24]. The band at 2069 cm<sup>-1</sup>, ascribed to linear carbonyl species, and at 1881 cm<sup>-1</sup>, due to bridging carbonyls, both adsorbed on metallic rhodium particles. Clearly, the linear Rh<sup>0</sup>-CO species prevailed on the reduced sample. Similar CO adsorption bands were observed after exposure to N<sub>2</sub>O. The linear Rh<sup>0</sup>-CO species continued to be the major adsorption state of CO, with some weak adsorption of gem-dicarbonyl Rh<sup>δ+</sup> and bridged carbonyl species as well. The general trend observed with increasing adsorption temperature of N<sub>2</sub>O was that linear carbonyls species remained unchanged. One possible reason is that Rh<sup>0</sup> species exhibited a good stability under reaction conditions. Besides that, the RhO<sub>x</sub> species formed during the N<sub>2</sub>O adsorption were unstable and easily reduced in the vacuum pre-treatment. However, as shown in Fig. 8B, the Rh/γ-Al<sub>2</sub>O<sub>3</sub> mainly comprised of Rh<sup>δ+</sup>(CO)<sub>2</sub> species. This information allows us to conclude that the silica-stabilized alumina favors the stabilization of Rh<sup>0</sup> species and further suggests that Rh<sup>0</sup> species are the active sites in the decomposition of N<sub>2</sub>O.

In order to obtain a clear understanding of the effect of silica doping on the oxygen mobility, adsorption microcalorimetry of O<sub>2</sub> was accomplished on the samples.

**Fig. 8** FT-IR spectra of the Rh/Si<sub>0.19</sub>Al (A) and the Rh/ $\gamma$ -Al<sub>2</sub>O<sub>3</sub> (B) samples arising from CO adsorption at room temperature submitted to the following pretreatments: fresh catalysts (a); reduced at 500 °C in hydrogen (b); and outgassed at 25 °C after treatment with N<sub>2</sub>O: at 100 °C (c), at 200 °C (d), at 300 °C (e), at 400 °C (f)

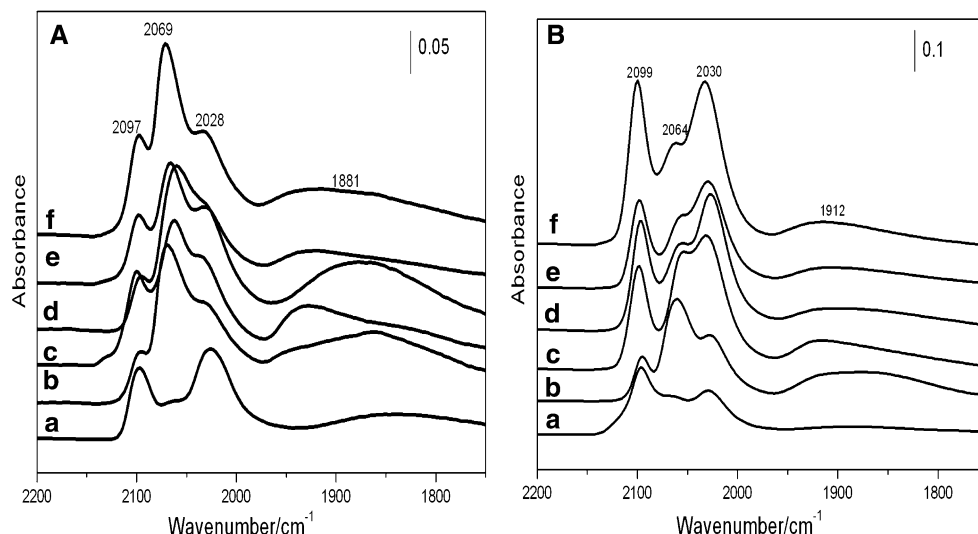
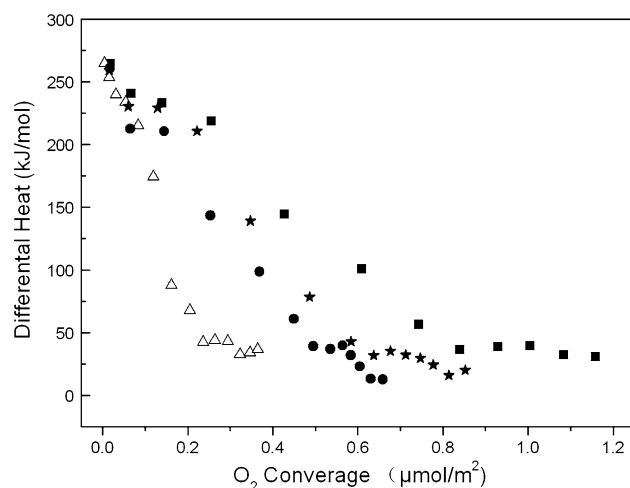


Figure 9 shows the oxygen adsorption volumetric isotherms on the silica-stabilized samples. Prior to O<sub>2</sub> adsorption, the samples were reduced with H<sub>2</sub> and then saturated with N<sub>2</sub>O. The initial differential heats of O<sub>2</sub> adsorption on the four samples were quite similar, around 264 kJ/mol. However, the capacity of oxygen adsorption of the Rh/Si<sub>0.05</sub>Al, Rh/Si<sub>0.19</sub>Al, Rh/Si<sub>0.32</sub>Al, and Rh/ $\gamma$ -Al<sub>2</sub>O<sub>3</sub> catalysts were 0.58, 0.79, 0.44, and 0.25  $\mu\text{mol}/\text{m}^2$ , respectively, well in accordance with the activity sequence of the catalysts. These results showed that there were more O<sub>2</sub> adsorption sites on the Rh/Si<sub>0.19</sub>Al catalyst than those of the other Rh catalysts. It should be noted that some of the adsorption sites on the catalyst have been occupied by the oxygen generated in the N<sub>2</sub>O decomposition during the



**Fig. 9** Differential heat of O<sub>2</sub> adsorption as a function of O<sub>2</sub> coverage on Rh catalysts: Rh/Si<sub>0.19</sub>Al (filled square), Rh/Si<sub>0.05</sub>Al (filled asterisk), Rh/Si<sub>0.32</sub>Al (filled circle), Rh/ $\gamma$ -Al<sub>2</sub>O<sub>3</sub> (open triangle). The samples were reduced with H<sub>2</sub> and then saturated with N<sub>2</sub>O prior to O<sub>2</sub> adsorption

N<sub>2</sub>O pre-adsorption process. Thus, the O<sub>2</sub> adsorption in this case could be regarded as the reversible oxygen adsorption, which directly reflected the migrating ability of oxygen on the catalyst.

Owing to a process of dehydroxylation in the phase transformation, oxygen vacancies are the most abundant in Si<sub>0.19</sub>Al, which greatly facilitates the migration of oxygen species from the active sites to the support favoring its final desorption from the catalyst [25]. Therefore, the support structure may be responsible for the great capacity of oxygen adsorption of the Rh/Si<sub>0.19</sub>Al. It has been mentioned previously that oxygen desorbing from the catalyst surface is the rate determining step for N<sub>2</sub>O decomposition. Therefore, the oxygen migrating ability of the Rh/Si<sub>0.19</sub>Al was thus assumed to be one main reason for the activity enhancement of N<sub>2</sub>O decomposition.

### 3.5 Thermal Stability of the Rh/Si<sub>x</sub>Al Catalysts

The thermal stabilization of a catalyst is another key parameter for evaluating its feasibility in the decomposition of N<sub>2</sub>O as a propellant. Figure 10 presents the N<sub>2</sub>O conversions of the Rh supported catalysts calcined at 1200 °C. The activity of the alumina supported catalyst was decreased dramatically after calcination at 1200 °C, with the N<sub>2</sub>O conversion of 20% at 600 °C, which could be correlated with the phase transformation of alumina and the sintering and/or vaporization of active components. In contrast, the Rh/Si<sub>x</sub>Al catalysts were only slightly affected by this treatment. Even after calcination at 1200 °C, the Rh/Si<sub>0.19</sub>Al catalyst still initiated the N<sub>2</sub>O decomposition at 350 °C and attained 95% conversion at 500 °C. It appears that the doping of silica not only strongly enhanced the catalytic activity of the Rh/Al<sub>2</sub>O<sub>3</sub> catalyst, but also significantly improved the thermal stability of the catalyst.

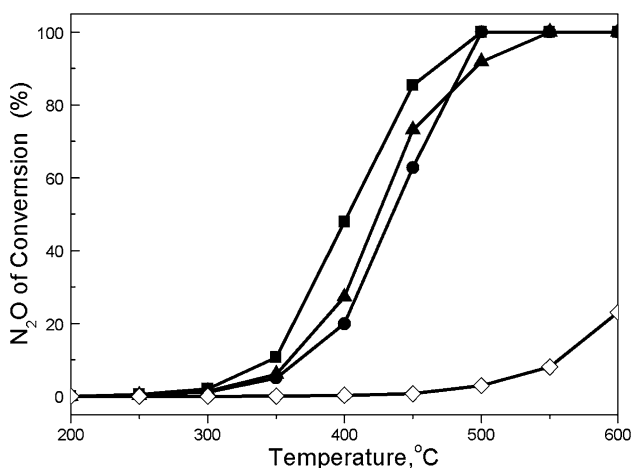


**Fig. 10** N<sub>2</sub>O conversion as a function of temperature over the Rh/Si<sub>x</sub>Al catalysts calcined at 1200 °C: 1200-Rh/Si<sub>0.19</sub>Al (filled square), 1200-Rh/Si<sub>0.05</sub>Al (filled triangle), 1200-Rh/Si<sub>0.32</sub>Al (filled circle), 1200-Rh/Al<sub>2</sub>O<sub>3</sub> (open diamond)

#### 4 Conclusion

Alumina modified with silica showed a great enhancement in the activity of N<sub>2</sub>O decomposition over the Rh catalyst supported thereof. The silica doping favors the stabilization of Rh<sup>0</sup> species and the desorption of oxygen species under reaction conditions. It can be concluded that the doping of alumina with silica is an effective way to improve the catalytic activity of N<sub>2</sub>O decomposition for propellant applications: an excellent catalytic activity at low temperatures associated with a high-temperature stability.

**Acknowledgments** Supports from Natural Science Foundation of China (NSFC, No. 20973165 and No. 20773122) and External Cooperation Program of Chinese Academy of Science (GJHZ200827) are gratefully acknowledged.

#### References

1. Zakirov V, Sweeting M, Goeman V, Lawrence T (2000) In: Proceeding of the 14th annual AIAA/USU conference on small satellites, USA, 21–24 Aug

2. Cong Y, Lv F, Yang TZ, Wang XD, Zhang T (2008) In: Space propulsion 2008, Greece, 5–9 May
3. Wallbank JR, Sermon PA, Baker AM, Courtney L, Sambrook RM (2004) In: Space propulsion 2004, Italy, 7–8 June
4. Zakirov V, Sweeting MN (2001) In: 37th AIAA/ASME/SAE/ASEE joint propulsion conference, The United States, 8–11 July
5. Navarro RM, Álvarez-Galván MC, Rosa F, Fierro JLG (2006) Appl Catal A 297:60
6. Álvarez-Galván MC, Navarro RM, Rosa F, Briceño Y, Gordillo AF, Fierro JLG (2008) Int J Hydrogen Energy 33:652
7. Schaper H, Doesburg EBM, van Reijen LL (1983) Appl Catal 7:211
8. Kim DH, Kwak JH, Szanyi J, Burton SD, Peden CHF (2007) Appl Catal B 72:233
9. Beguin B, Garbowski E, Primet M (1991) Appl Catal 75:119
10. Courthéoux L, Popa F, Gautron E, Rossignol S, Kappenstein C (2004) J Non-Cryst Solids 350:113
11. Wang X, Guo Y, Lu G, Hu Y, Jiang L, Guo Y, Zhang Z (2007) Catal Today 126:369
12. Horiuchi T, Osaki T, Sugiyama T, Suzuki K, Mori T (2001) J Non-Cryst Solids 291:187
13. Osaki T, Nagashima K, Watari K, Tajiri K (2007) J Non-Cryst Solids 353:2436
14. Zhao XY, Cong Y, Lv F, Li L, Wang XD, Zhang T (2010) Chem Commun 46:3028
15. Zhu SM, Wang XD, Wang AQ, Cong Y, Zhang T (2007) Chem Commun 1695
16. Tian M, Wang AQ, Wang XD, Zhu YY, Zhang T (2009) Appl Catal B 92:437
17. Arai H, Machida M (1996) Appl Catal A 138:161
18. Rossignol S, Kappenstein C (2001) Int J Inorg Mater 3:5
19. Kondratenko EV, Kondratenko VA, Santiago M, Pérez-Ramírez J (2008) J Catal 256:248
20. Imamura S, Tadani J, Saito Y, Okamoto Y, Jindai H, Kaito C (2001) Appl Catal A 201:121
21. Hwang CP, Yeh CT, Zhu Q (1999) Catal Today 51:93
22. Paul DK, Marten CD Jr, Yates JT (1999) Langmuir 15:4508
23. Yates JT Jr, Duncan TM, Vaughan RW (1979) J Chem Phys 71:3908
24. Basu P, Panayotov D, Yates JT Jr (1988) J Am Chem Soc 110:2074
25. Drago RS, Jurczyk K, Kob N (1997) Appl Catal B 13:69